ECS Transactions, 19 (3) 321-328 (2009)
10.1149/1.3120712 ©The Electrochemical Society

Simulating Crystallographic Pore Growth in III-V semiconductors

M. Leisner, J. Carstensen, and H. Föll

Institute for Materials Science, Christian-Albrechts-University of Kiel
Kaiserstrasse 2, 24143 Kiel, Germany

In this work, the growth of crystallographically oriented pores in III-V semiconductors has been investigated. Based on new and previous results a model for pore growth has been developed, which is mainly based on a stochastic branching probability of the pores. The stochastic nature of the model allowed to implement it as the core for Monte-Carlo-Simulations of pore growth. The simulations were able to reproduce the main features of crystallographically oriented pores, like uniform pore growth in n-type InP or the formation of domains on n-type GaAs and InP. The model is also capable of reproducing the logarithmic growth law for the pore depth, as well as the pore density oscillations with depth, as recently found.

Introduction

Electrochemical pore growth on III-V semiconductors can be basically classified into two groups according to the resulting pore morphologies. Most attention has been focused on the so-called current-line oriented pores ("Curros"). These pores are typically non-facetted. i.e. they have smooth pore walls with often cylindrical cross-sections and always grow perpendicular to the equipotential lines, i.e. usually perpendicular to the surface, independent of the substrate's crystallographic orientation (1 - 5). Curros so far have been observed in n-type InP, as well as in GaP and Si; in GaAs no curros have yet been found. As shown by Tiginyanu et al. (6), pores on II-VI semiconductors like CdSe show striking similarities to pores found in III-V's and might thus also fall into this class of pores. The second kind of pores are crystallographically oriented pores ("Crystos") (2, 7, 8). These pores always grow into <111>B directions, and often are heavily facetted with a triangular cross-section, and pore tips and pore walls composed from {111} planes (for details see (9)). Crysto pores have been observed in Si and Ge but particularly in n-type InP, GaAs, and GaP, even though it is difficult to nucleate crysto pores homogeneously on the latter two semiconductors (10). Crysto pores are rather unsensitive to the electrolyte used. The standard electrolyte for pore etching in III-V's is based on HCl, but similar crysto pores can be obtained for electrolytes like KOH (11, 12) or "salt water" (6).

While a considerable amount of work has been spent on electrochemical pore growth in III-V semiconductors, the understanding of the growth mechanisms still remains patchy. In this work, a model for the growth of crysto pores in III-V's is developed, which is mainly based on a stochastic process of pore branching, i.e it is of the "current burst" type (13). This allows implementing the model with a Monte-Carlo approach in a three-dimensional array of voxels. Results of the model are compared to dedicated experiments undertaken for this purpose and to older results either not fully appreciated or not fully understood in the past.

Experimental

Pore Etching

Samples consisted of single-crystalline (100)-oriented n-type InP, with a doping concentration $N_D = 10^{17}$ cm^{-3}, as well as of (100)-oriented n-type GaAs with a doping concentration $N_D = 10^{17}$ cm^{-3}. The sample size was $A = 0.25$ cm^2. Experiments have been performed in the electrochemical double-cell described in full detail in (14). Aqueous HCl with a concentration of 5 wt. % (= 1.4 M) has been used as electrolyte. All experiments have been performed under constant-current conditions at a constant temperature of $T = 20$ °C.

Monte-Carlo-Simulations

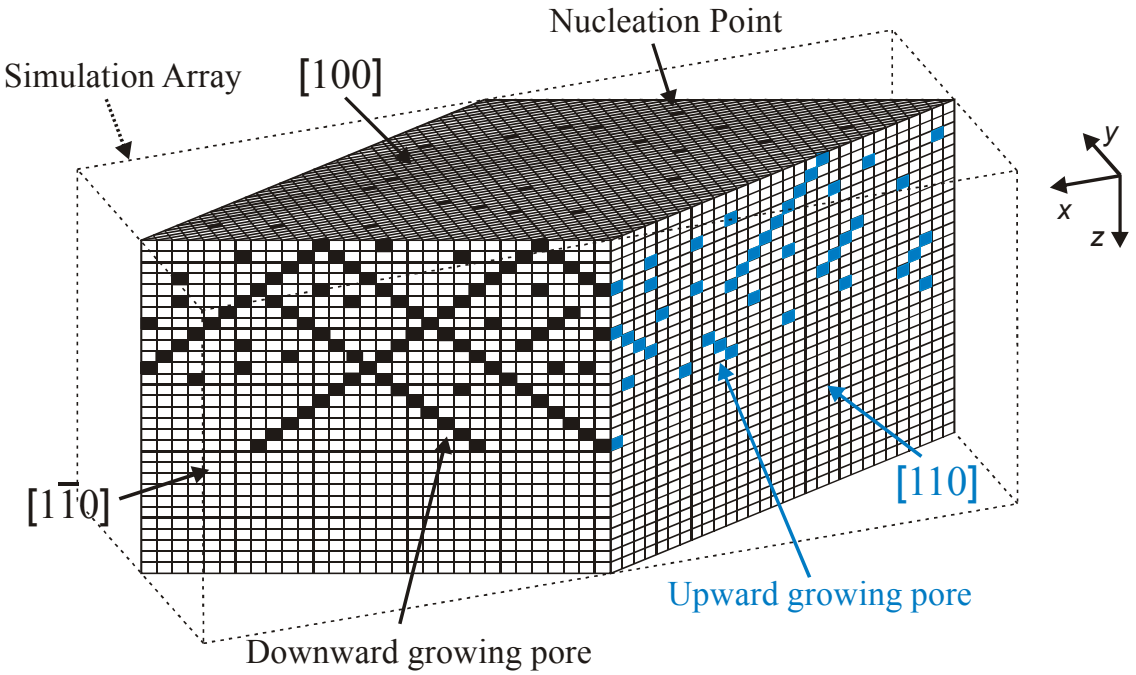

Figure 1: Schematic illustration of the simulation array. On top the nuclei or nucleation points that lead to downward growing pores are illustrated (left-hand part). All pores can branch at the tips or from a pore wall. Pores growing into the depth are shown as a succession of black squares on the front view (left-hand part), while upwardly growing pores show up as isolated back squares. On the side view (right-hand part) the situation is reverse.

Based on previous results and models from our group, in particular the current burst model for pore growth and self-induced oscillations (13), a three-dimensional model has been specifically developed that allows Monte-Carlo-Simulations of crysto pore growth in III-V semiconductors. In these simulations, an array of $(1024)^3 = 1.07 \cdot 10^9$ voxels has been used, with a mesh size set to 100 nm, corresponding to the experimentally determined typical crysto pore size. The top layer of this array is filled with nucleation seeds for the crysto pores in some distribution and density as a starting condition. The

nuclei density, the depth of the nucleation layer, and the kind of nuclei distribution (random, periodic,...) can be freely chosen.

As illustrated in Fig. 1, after nucleation has taken place, the pores begin to grow one voxel into the two downward oriented <111>B directions with every iteration cycle. As observed experimentally, the pores are able to branch in two different ways. A pore can branch at the tip into the other downward oriented <111>B direction, or a new pore tip can branch out of the previously etched pore walls into one of the two upward oriented <111>B directions. The upward growing pores are then also able to branch similar to the downward growing pores.

The key point of the model is that certain different branching probabilities k_{tips} and k_{walls}, respectively, are attributed to both branching processes. In addition, an adjustable length of the pore in the order of the space charge region (SCR) width d_{SCR}, measured from its point of generation by branching will be assigned $k = 0$, i.e. it will not be able to form branches on that length because as long as the SCRs overlap the new tip cannot experience the full voltage drop. In a last primary point it is assumed that all pores stop to grow if other pores block their trajectory. In other words, pores cannot grow through the space-charge-region surrounding other pores.

The model then needs two more basic but reasonable assumptions:

1. The dissolution valence is constant.
2. The two different branching probabilities are both proportional to the current density j_{tips} at the pore tips.

This is sufficient to run the Monte Carlo simulation. Note that while the probability of branching is constant, the generation rate of pores may vary because for pores formed by branching from a pore wall it is proportional to the pore length and that increases the rate with time, while the proportionality to the current decreases both rates since j_{tips} decreases as the number of tips increases.

Results

Homogeneous Crysto Pore Structures on InP

Etching homogeneous layers of crysto pores in n-type InP can be best achieved by performing constant current experiments and applying the conditions as outlined in the experimental section. For a (comparatively low) current density j = 0.4 mA/cm^2 pore structures as illustrated in Fig. 2a result after an etching time of 240 min. One can easily observe the upward growing crysto pores as straight lines in this cross-sectional SEM micrograph; the downward growing pores intersect the cleavage plane and appear as triangles. The inset shows details at higher magnification. Fig. 2b shows a result from the Monte-Carlo-Simulation, which has been obtained for an adequate set of model parameters (Nucleation tip density: 0.09 µm^{-2}, randomly distibuted, current density: 0.4 mA/cm^2, starting branching probability walls: 0.003, starting branching probability tips: 0.3, starting velocity: 2.5 µm/min). Note that the triangles are shown as quadratic pixels in the simulation pictures. It can be stated, that there is a fairly good agreement of the resulting pore structures.

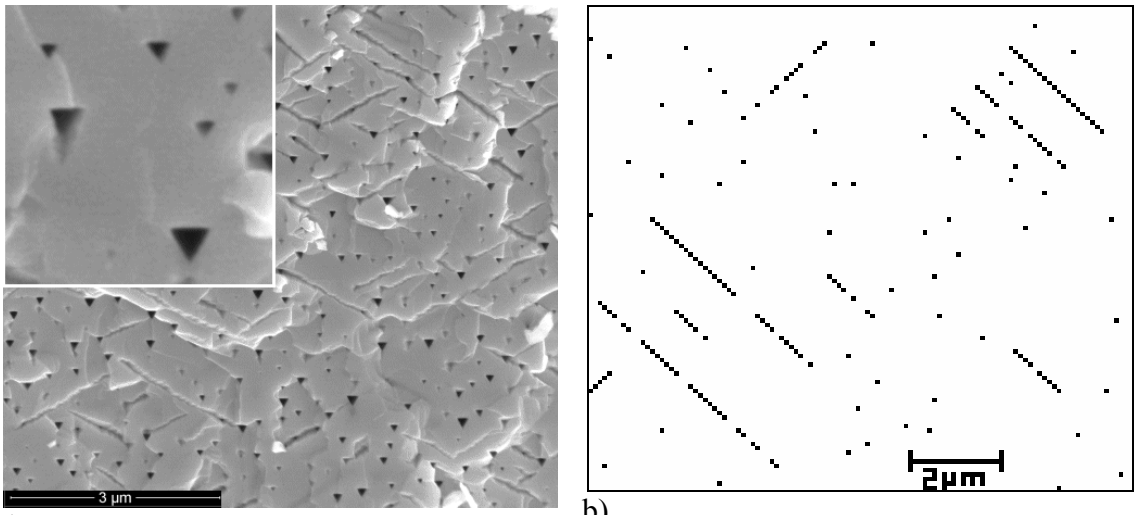

a) b)

Figure 2: Comparison of experimental and simulated pore structures. a) Crysto pore structure obtained after etching galvanostatically at j = 0.4 mA/cm^2 for 240 min. b) Directly comparable crysto pore structure obtained from the Monte-Carlo-Simulation for an adequate set of parameters.

For the same conditions as before, several experiments with different etching times have been performed. The depth of the etched porous layers has been determined from SEM pictures. The resulting pore depth vs. time is plotted in Fig. 3 (black squares). A logarithmic growth law can describe the functionality:

$$d_{pore} \propto \ln t\,. \qquad [1]$$

The solid line in Fig. 3 represents the result from Monte-Carlo-Simulations with one set of paramters; it matches the experimentally determined data very well. Theoretically, the logarithmic growth law is a direct consequence of the main assumptions of the model, i.e. of the proportionality of the pore branching to the current density at the pore tips (15). The fact that the simulation yields the observed growth law not only lends credibility to the model, but also confirms that the model is properly implemented in the simulations. The same line of reasoning applies to the number of pore tips as a function of time (not shown here). From the model a linear dependence is expected, which the simulation yields as well.

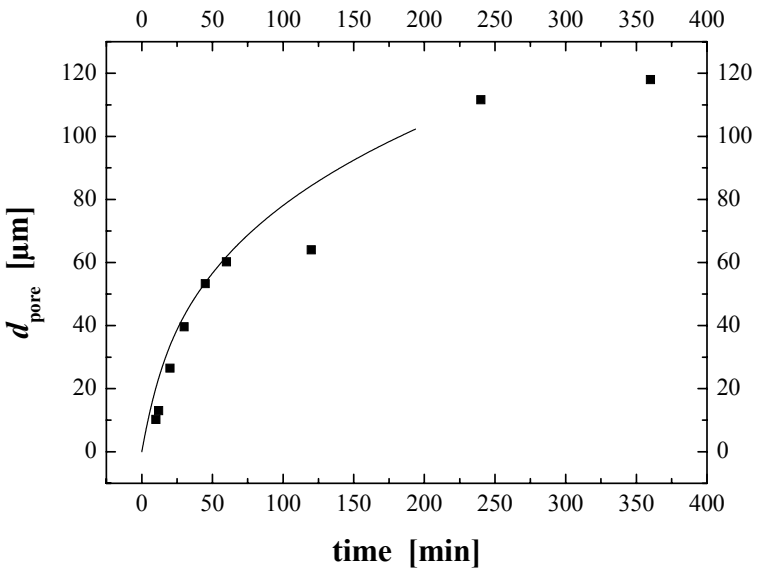

Figure 3: InP crysto pore depth as a function of etching time. Black squares represent the experimentally determined data. The line is the result from the Monte-Carlo-Simulations.

A rather surprising result has been obtained for the pore density as a function of depth. This quantity has been determined from cross-sectional SEM micrographs. The density is not monotonously decreasing, as one would intuitively expect, it is showing sinusoidal oscillations with a wavelength in the range between (6 – 10) µm, as can be seen in Fig. 4a. The Monte-Carlo-Simulations reproduced the effect partially, as shown in Fig 4b. A closer look at previous work revealed that these oscillations have already been observed, but not been recognized, in the TEM investigations published in (9).

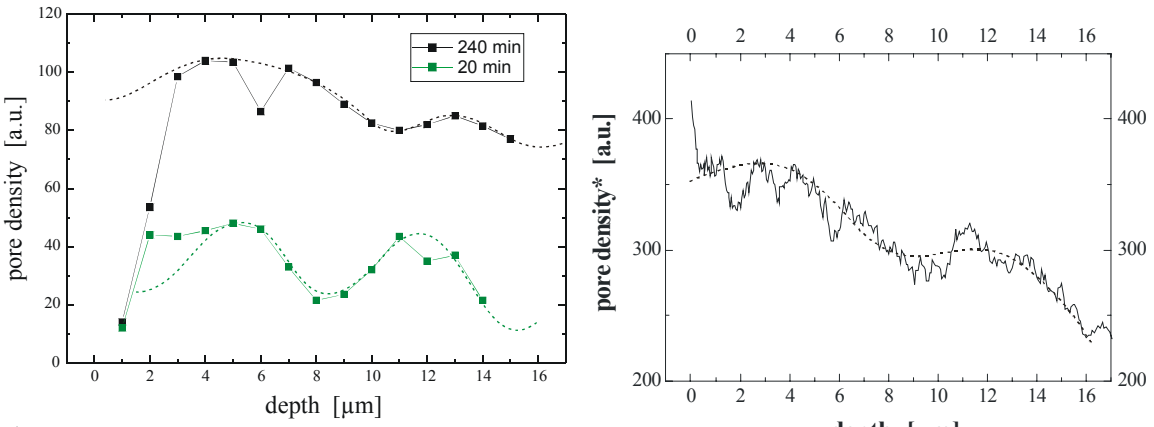

a) b)

Figure 4: InP crysto pore density as a function of depth. a) Results from the dedicated etching experiments. b) Results from the Monte-Carlo-Simulations. For an explanation of the oscillatory behavior see the text.

This simulation of crysto pore growth should also be possible for GaAs and GaP, after adjusting model parameters like mesh size, current density, and in particular the nucleation.

Pore Domains on GaAs and InP

As has been shown in (2), domain structures can be obtained on n-type GaAs and InP. The formation of domains mainly relies on the nucleation conditions, i.e. a rather low nucleation density is necessary. In combination with high constant current conditions (j = 80 mA/cm^2 here), it will lead to strong branching and formation of the domain structure in short times. Fig. 5a gives an example of a domain grown on GaAs as seen in a SEM surface view. The initial pore pair starts to grow in the center of the square and strong branching subsequently leads to upward growing pores, which will eventually reach the surface again, and thus form the pore domain as shown in Fig. 5a. A closer look at the domain surface reveals that 4 quadrants exist, 2 triangles with a higher pore density and 2 triangles with a lower pore density. For a comprehensive illustration of this effect see reference (2). Fig. 5b shows the corresponding result from the Monte-Carlo-Simulations(Nucleation tip density: 0.0004 µm^{-2}, randomly distibuted, starting branching probability walls: 0.5, starting branching probability tips: 0.5, starting velocity: 2.5 µm/min).. The similarity to the experimental results is striking; even the 4 triangles and the line-up of the pores in two of them are clearly visible.

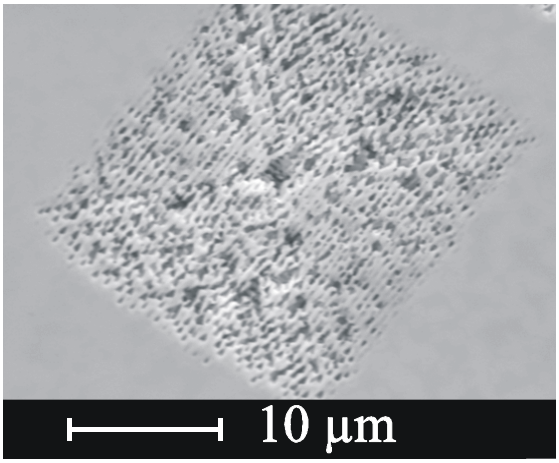

a)

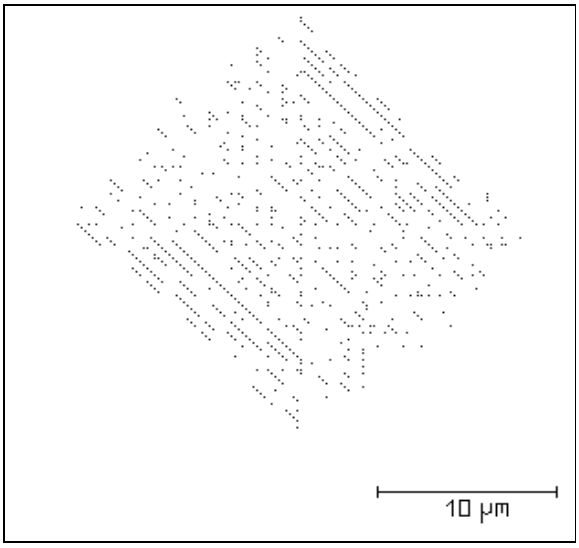

b)

Figure 5: Crysto pore domains in GaAs. a) SEM surface view of a crysto pore domain. Constant current experiment: j = 80 mA/cm^2, electrolyte concentration 5 wt.% HCl aq. b) Corresponding results from the Monte-Carlo-Simulations.

Discussion

The relatively simple model, with two basic assumptions, which has been implemented into Monte-Carlo-Simulations, is able to reproduce different experimentally observed crysto pore structures on different III-V semiconductors, like homogeneous pore layers on n-type InP and the phenomenon of domain formation on n-type GaAs and InP. The main simulation parameters, used to achieve the different pore structures, are the branching probabilities at the pore tips and pore walls. The images of the simulation results shown in Figs. 2 and 5 show a very good agreement to the experimentally found pore structures observed in the corresponding SEM micrographs.

For the time dependence of the pore depth, the simulation yields the logarithmic growth law, which very well matches the experimentally found results. This is expected, since the model was designed to result in a logarithmic pore depth growth. The same holds for the number of pore tips as function of etching time, a linear relationship is observed in the simulations, as is theoretically expected from the model. Still both results strongly indicate, that the model is a valid description of crysto pore growth on III-V semiconductors.

For the pore density as function of depth, the interesting oscillations shown in Fig. 4 have been found in good agreement to the results of the simulation. The strength of a simulation is the full access to all parameters as a function of time at all positions which could never be measured in such detail. This allows an investigation of the origin of the pore density oscillation, which can be summarized as follows: The density oscillations occur, because in a certain depth a critical pore density is reached, so that no further branching is possible, since all free space between the pores is covered by space charge regions. Thus, some pore tips die out and will hence increase the current density at the pore tips. In the framework of the model this will lead to enhanced branching probabilities at the tips and walls. Since this branching can only occur at some distance to the region where the critical pore density has already been obtained, an intrinsic length scale is introduced, which will define the wavelength of the oscillations. Geometrically this length scale is defined by the (average) distance of nucleation sites at the surface and the angle of the first <111> pores growing into the depth.

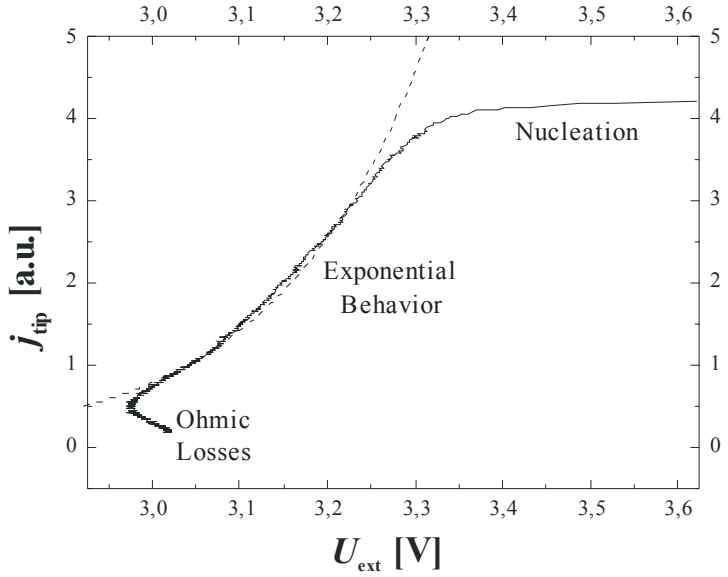

Figure 6: Pseudo IV Curve for crysto pore growth on n-type InP. The curve is constructed out of simulation ($j_{tips}(t)$) and experimental data ($U(t)$). For details see the text.

The strongest assumption in the model is that at all pore tips (up-growing, down-growing, branched) the same current density is flowing. In the following we will combine the data extracted from the simulation with the measured $U(t)$ data to check, if the assumption is valid and which further consequences follow from the assumption. Thus, dividing the externally flowing constant current by the number of pore tips, resulting from the Monte-Carlo-Simulation, will yield the time development of $j_{tips}(t)$ during an experiment. Since

the time development of the voltage is directly measured in the experiments, it is possible to construct a "pseudo IV curve" by combining the simulation data ($j_{tips}(t)$) and the experimental data ($U(t)$). Fig. 6 shows the resulting "pseudo IV curve". In the main part of the etching experiment an exponential behavior is found (as indicated by the dashed line), which is a strong hint that simple Butler-Vollmer kinetics dominates the etching processes at all pore tips. In the nucleation phase the behavior deviates from the exponential behavior, which is expected, since the real nucleation is probably far more complicated than the approach in the simulations. Towards the end of the experiment the curve also deviates. A possible explanation for this phenomenon might be that the ohmic losses due to the increase in pore length have been ignored so far. To get the correct voltage at the pore tips the ohmic losses can be calculated from the simulation of the pore geometry as a function of time, i.e. the (average) pore length has to be calculated from the pore length distribution during pore growth. If these results would correct the dip in the IV curve, it would be a further strong indication for the validity of the model for crysto pore growth in III-V semiconductors.

References

1. E. Kikuno, M. Amiotti, T. Takizawa, and S. Arai, *Japan J. Appl. Phys.* **34(1, 1)**, 177 (1995).
2. H. Föll, S. Langa, J. Carstensen, S. Lölkes, M. Christophersen, and I.M. Tiginyanu, *Adv. Mater.* **15(3)**, 183 (2003).
3. H. Hasegawa and T. Sato, *Electrochim. Acta* **50**, 3015 (2005).
4. P. Schmuki, U. Schlierf, T. Herrmann, and G. Champion, *Electrochim. Acta* **48**, 1301 (2003).
5. A.M. Gonçalves, L. Santinacci, A. Eb, I. Gerard, C. Mathieu, and A. Etcheberry, *Electrochem. Solid-State Lett.* **10(4)**, D35 (2007).
6. I.M. Tiginyanu, V.V. Ursaki, E. Monaico, E. Foca, and H. Föll, *Electrochem. and Sol. State Lett.* **10(11)**, D127 (2007).
7. T. Takizawa, S. Arai, and M. Nakahara, *Japan J. Appl. Phys.* **33(2, 5A)**, L643 (1994).
8. H. Tsuchiya, M. Hueppe, T. Djenizian, P. Schmuki, and S. Fujimoto, *Sci. Technol. Adv. Mater.* **5**, 119 (2004).
9. E. Spiecker, M. Rudel, W. Jäger, M. Leisner, and H. Föll, *Phys. Stat. Sol. (a)* **202(15)**, 2950 (2005).
10. S. Langa, J. Carstensen, M. Christophersen, K. Steen, S. Frey, I.M. Tiginyanu, and H. Föll, *J. Electrochem. Soc.* **152(8)**, C525 (2005).
11. C. O'Dwyer, D.N. Buckley, D. Sutton, and S.B. Newcomb, *J. Electrochem. Soc.* **153(12)**, G1039 (2006).
12. C. O'Dwyer, D.N. Buckley, D. Sutton, M. Serantoni, and S.B. Newcomb, *J. Electrochem. Soc.* **154(2)**, H78 (2007).
13. J. Carstensen, R. Prange, G.S. Popkirov, and H. Föll, *Appl. Phys. A* **67(4)**, 459 (1998).
14. S. Langa, I.M. Tiginyanu, J. Carstensen, M. Christophersen, and H. Föll, *Electrochem. Solid-State Lett.* **3(11)**, 514 (2000).
15. M. Leisner, J. Carstensen, A. Cojocaru, and H. Föll, *ECS Trans.* **16(3)**, 133 (2008).